

Investigation of Shannon Entropy and Minimum Entropy Changes Across the Entire Brain Frequency Spectrum and by Individual Brainwave Bands in Faradarmangars

Mohammad Ali Taheri¹, Sara Torabi², Farid Semsarha^{3*}

* Corresponding author: Farid Semsarha Ph.D., Institute of Biochemistry and Biophysics (IBB), University of Tehran,

P.O. Box: 13145-1384, Tehran, Iran

Tel.: +98-9121786577

Email: Semsarha@ut.ac.ir

1. Sciencefact R&D Department, Cosmointel Inc.

Research Center, Ontario, Canada

2. Department of Plant Biology, School of Biology,

College of sciences, University of Tehran, Tehran, Iran

3. Institute of Biochemistry and Biophysics (IBB),

University of Tehran, Tehran, Iran

DOI: <https://doi.org/10.61450/joci.v4i19.227>

Abstract

The Faradarmani Consciousness Field, which is a subset of the Cosmic Consciousness Network, is non-physical in nature. Although its characteristics cannot be identified using quantitative instruments, it is possible to detect its effects through experimental design. In this context, the brain's response under the influence of this field has been investigated in previous studies, and changes in electrical activity have been recorded. It is hypothesized that information transmitted under the influence of this field leads to observable changes at the brain level. Based on information theory introduced by Shannon, entropy calculation provides a quantitative measure of the information content within the data. Accordingly, this study assessed two types of entropy, Shannon entropy and minimum entropy, based on total absolute power and absolute power across various brainwave frequency bands. It is worth noting that although entropy has been examined in previous studies related to consciousness fields in other contexts, this is the first time it has been applied to brain electrical activity. According to the findings, both Shannon and minimum entropy of total brain activity decreased under the influence of the Faradarmani Consciousness Field, which may serve as a meaningful indicator of its impact on the brain and its electrical activity. From a frequency-based perspective, this entropy reduction, in terms of Shannon entropy, was observed across all frequency bands at the onset of using the Faradarmani Consciousness Field (Task 1), while the reduction in minimum entropy was seen in all bands except high beta and gamma 1.

Keywords: Shannon entropy, minimum entropy, brain waves, Faradarmani Consciousness Field

Introduction

Information theory, introduced by Claude Shannon in 1948, provides a mathematical framework for quantifying the amount of information in data by measuring uncertainty and the efficiency of information transmission (Shannon, 1948). One of the central concepts in information theory is entropy, which measures the degree of disorder or unpredictability within a system (Saraiva, 2023). In the context of EEG (electroencephalography) experiments, information theory is an essential tool for analyzing brain wave patterns and understanding brain activity (Bein, 2006). By calculating Shannon entropy, researchers can assess the complexity of neural signals and quantify the information processed by the brain (Keshmiri, 2020).

In studies examining tinnitus, entropy calculations have been shown to reveal differences in brain activity between healthy individuals and those suffering from chronic tinnitus, highlighting the role of increased entropy in reflecting the chaotic behavior of the brain (Sadeghijam et al., 2021). Similarly, entropy-based analysis has shown promise in distinguishing individuals with schizophrenia from healthy controls (Sabeti et al., 2009).

According to Taheri, Consciousness is not a product of brain activity; rather, it is a fundamental element of the universe from which information, matter, and energy originate. He coined the term T-Consciousness to distinguish his viewpoint from other theoretical concepts. In this framework, various T-Consciousness Fields exist as subcategories of the Cosmic Consciousness Network. The Faradarmani Consciousness Field is one such field (Taheri, 2013). Its effect is initiated by a brief moment of attention through the human mind. It is hypothesized that information transmitted from this field can lead to detectable changes in brain activity.

Such changes have been reported in previous experiments (Taheri et al., 2022; Taheri et

al., 2022a). In the current study, based on Information Theory, alterations in entropy values were calculated using data from the entire brain frequency spectrum and specific brain wave bands, to estimate changes in information content under the influence of the Faradarmani Consciousness Field.

Method

Forty-four healthy adult participants (mean age: 41 ± 7 years), none of whom had used any neurological or psychiatric medications in the six months prior to the test day, were included in the study group. Of these participants, 41% were male ($n=18$) and 59% were female ($n=26$). The Faradarmani Consciousness Field treatment was initiated by the participants at a predetermined time (upon hearing a soft beep sound from the computer system located on the desk in front of the seating area). In this study, a task referred to the action in which Faradarmangars personally initiated a connection with the Cosmic Consciousness Network. The study was approved by the Ethics Committee of Iran University of Medical Sciences (Approval ID: IR.IUMS.REC.1402.940).

The time intervals were defined as follows:

1. Rest 1: In this stage, the trained participants, referred to as *Faradarmangars*, were asked not to engage any type of T-Consciousness Fields and to remain simply relaxed and tension-free. The aim of this stage was to collect baseline data for each individual as a control before applying the FCF, which is useful for creating a collective control dataset.
2. Task: At the beginning of Rest 1, upon hearing the sound of a horn, predefined before the experiment, the participants initiated their connection with the FCF, marking the beginning of Task 1. In fact, the task involved a continuous connection for 10 minutes. During this stage, data was continuously collected from the participants' brains. In the analysis phase, the data was

examined both as a whole and in three equal, consecutive intervals, referred to as Task 1, Task 2, and Task 3. The purpose of this segmented analysis was to evaluate how the FCF affects the brain over time.

3. Rest 2: Another three-minute stage followed, during which the participants disengaged from their connection with the FCF upon hearing the second horn sound, as defined prior to the experiment. Similar to Rest 1, they remained relaxed and tension-free without using the FCF.

EEG data acquisition

The participants' brain electrical activity was recorded at the National Brain Mapping Laboratory (NBML) of Iran using the g.tec g.HIamp system (g.tec, Graz, Austria) with a 128-channel cap equipped with passive Ag/AgCl electrodes. The electrodes were evenly distributed across the scalp based on the international 10/20 system for electrode placement. The ground electrode was placed on the forehead, and the online reference was positioned on the right earlobe. Data was recorded with a sampling frequency of 512 Hz, and impedance was maintained below 10 k Ω .

Data Processing

The EEG data were preprocessed using the EEGLAB (Delorme and Makeig, 2004) and FieldTrip (Oostenveld et al., 2011) toolboxes for MATLAB (MATLAB R2016a, The MathWorks, Inc., Natick, MA, USA). High-pass filters (with a cutoff frequency of 2 Hz) and band-stop filters (to remove 50 Hz line noise and its harmonic frequencies) were applied to the raw data. The data were re-referenced to the common average reference, and artifacts were manually rejected through visual inspection using EEGLAB. Independent Component Analysis (ICA) was performed to remove artifact-related components (e.g., head and eye movements, heartbeat, and muscle tone). The preprocessed data, containing minimal artifacts, were segmented into different rest and task phases according to the study

design. FieldTrip was then used for further EEG data processing.

Frequency domain analysis is performed using the Fast Fourier Transform (FFT) algorithm (with a resolution of 0.125 Hz) to calculate the absolute power density ($\mu\text{V}^2/\text{Hz}$). The absolute power of a band is the integral of all power values within its frequency range. The mean (overall) frequency (Hz) is also obtained from the entire analyzed spectrum (1 to 30 Hz) (Yuvaraj et al., 2024).

Entropy Calculation

To assess entropy in this study, the absolute power values were used in the total state as well as separately for each individual frequency band. These values were binned with unit intervals, and the frequency of values generated in each bin was measured. Based on this, the frequency distribution entropy was calculated using the following Shannon equation (1):

$$1. \quad S = - \sum p_i \ln p_i$$

Where p_i is the probability of values occurring in the i th bin, and n_i is the number of values in that bin.

Additionally, the minimum entropy (2), which is a measure of the randomness of the generated values, is obtained using the following equation:

$$2. \quad S_{min} = - \log_2 P_{max}$$

Where P_{max} is the probability of the highest frequency in the distribution of the generated values.

Data analysis

Descriptive statistical analysis, frequency distribution analysis, and chart plotting were performed using GraphPad software version 9. Entropy calculations were carried out using SPSS software version 28. Differences between time-based populations were analyzed using two-way ANOVA. A p-value threshold of 0.05

was considered for significance; any change with a p-value less than this threshold was regarded as statistically significant, while changes above this value were considered non-significant (ns).

Results

The data related to the calculated Shannon entropy and minimum entropy values are presented in Tables 1 to 3, and the trends of their changes, normalized to the R1 values in each frequency range, are shown in Figures 1 to 6.

Table 1. Shannon entropy values in the frequency ranges of this study

Shannon Entropy					
Time Frame	1: R1	2: T1	3: T2	4: T3	5: R2
All	2.49	2.04	2.24	2.26	2.32
Delta	2.05	1.92	2.15	2.27	1.96
Tetha	2.87	2.43	2.62	2.67	2.33
Alpha1	2.37	2.00	2.22	2.26	2.36
Alpha2	2.50	1.97	2.20	2.08	2.45
Beta1	2.41	1.94	2.22	2.14	2.45
Beta2	2.72	2.45	2.65	2.67	2.80
Beta 3	2.34	2.16	2.32	2.33	2.36
High B	2.06	2.02	2.05	2.07	2.09
Gamma1	1.99	1.96	2.07	2.16	2.15
Gamma2	2.61	2.51	2.63	2.85	2.79

Table 2. Minimum entropy values in the frequency ranges of this study

Min Entropy					
Time Frame	1: R1	2: T1	3: T2	4: T3	5: R2
All	3.07	2.28	2.58	2.52	2.52
Delta	2.39	2.22	2.66	2.73	2.39
Tetha	3.39	2.81	3.17	3.17	2.58
Alpha1	2.81	2.33	2.73	2.45	2.58
Alpha2	2.45	1.89	2.22	2.07	2.45
Beta1	2.52	2.02	2.45	2.39	2.52
Beta2	2.98	2.89	3.17	2.98	3.39
Beta 3	2.81	2.39	2.58	2.73	2.89
High B	2.28	2.33	2.02	2.17	2.28
Gamma1	2.12	2.17	2.17	2.39	2.52
Gamma2	3.07	2.89	3.07	3.52	3.39

Table 3. Comparison of the percentage change in Shannon entropy values across different frequency ranges of the brain, compared to the R1 range (rest or control 1); colors similar to the total entropy indicate changes within $\pm 3\%$ of the total value. Smaller and aligned changes are shown in lighter green, while larger and aligned changes are shown in darker green. Red indicates changes that are not aligned with the total.

Shannon Entropy Change				
	T1-R1	T2-R1	T3-R1	R2-R1
All	-18.3604	-10.1577	-9.49575	-6.92812
Delta	-6.64923	4.960002	10.74217	-4.54802
Tetha	-15.1928	-8.48946	-6.79966	-18.7441
Alpha1	-15.6947	-6.34428	-4.97059	-0.58094
Alpha2	-21.229	-11.9004	-16.7901	-2.03418
Beta1	-19.5929	-7.83402	-11.2239	1.783805
Beta2	-9.73926	-2.55356	-1.5518	3.170758
Beta3	-7.80993	-0.55485	-0.47878	1.066345
Hbeta	-1.92068	-0.80133	0.385851	1.422277
Gamma1	-1.22172	3.894434	8.455378	8.231027
Gamma2	-3.91715	0.765034	9.098894	6.98985

R1: Rest 1, T1: Task 1, T2: Task3, R2: Rest2

As seen in Table 3, the only section with completely decreasing changes in Shannon entropy across all frequency ranges is the contrast related to Task 1. Additionally, in all contrasts of total absolute power, the Shannon entropy value is negative, with its maximum corresponding to the Task 1 and Rest 1 contrast, indicating that the values of Task 1 are about 18% lower than those of Rest 1. The start of changes in Rest 2, in the opposite direction to Task 1, begins from the Beta 1 frequency range, and the only section with negative Shannon entropy for Gamma waves is the contrast related to Task 1.

For Delta waves, a decrease in Shannon entropy is observed in Task 1 and Rest 2 in a similar manner. After the Theta range, where entropy changes in the different sections show a smaller decrease and align with Task 1, a distinct decrease in entropy is observed in the contrast of Rest 2 in the Alpha wave range (Alpha 1 and 2). Further, in the frequency range of Beta waves 1 to 3, a clear increase in entropy is observed in the contrast of Rest 2. From the High Beta range (starting boundary of Gamma) to the end (Gamma 1 and 2), a completely different entropy response in Task 1 compared to other sections is observed: in High Beta, Task 3 and

Rest 2 show an increase in entropy, and in both Gamma waves, Tasks 2 and 3, along with Rest 2 (all sections except the Task 1 contrast), show an increase in entropy. The trend of changes observed in minimum entropy is largely similar to the changes in Shannon entropy, with the difference that the increase in entropy in Rest 2 for high-frequency waves is only observed in Gamma waves, and Beta 1 wave shows a behavior similar to Alpha 2 in Rest 2.

The trend of changes normalized to the total absolute power of the R1 section across different brain wave ranges also provides insight into the entropy changes. Figure 1 shows the trend of changes for Delta and Theta waves. The trend of changes up to Task 3 is similar to the trend of total Shannon entropy changes, and even in the continuation and Rest 2 section, the decreasing trend continues. As shown in Figure 2, the trend of changes becomes closer to the trend of total Shannon entropy changes with an increase in wave speed. The Shannon entropy values in all waves in Rest 2 tend to approach those in Rest 1. According to Figure 3, among the high Beta and Gamma waves, the trend of changes in high Beta waves most closely resembles the trend of

total Shannon entropy changes, and in Rest 2, it tends to approach the values seen in Rest 1.

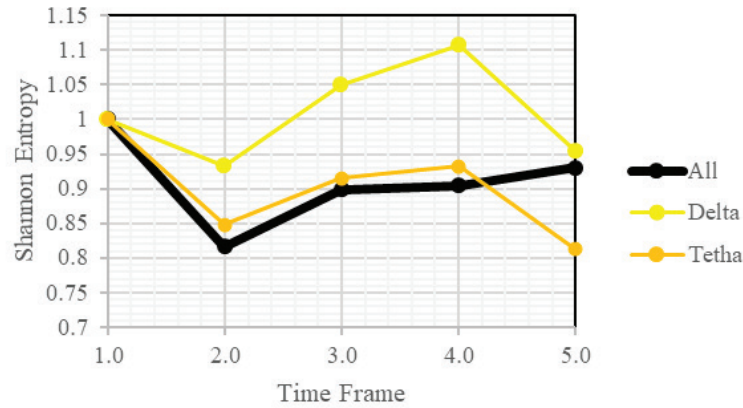


Figure 1. The trend of changes normalized to the total absolute power of the R1 section, compared to the two frequency ranges with the minimum brain wave speeds (Delta and Theta). 1: Rest 1, 2: Task 1, 3: Task 2, 4: Task 3, 5: Rest 2.

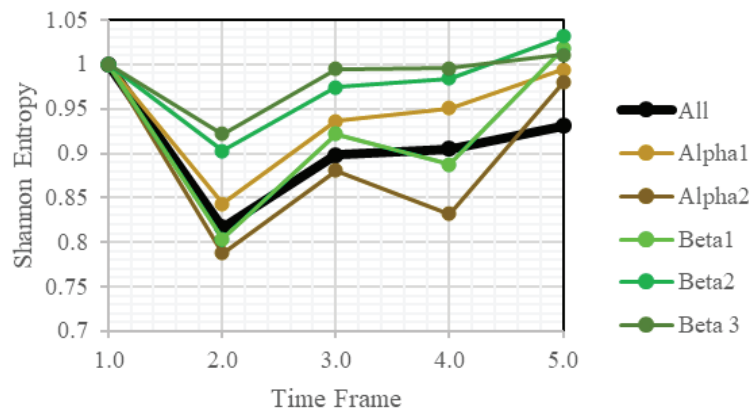


Figure 2. The trend of changes normalized to the total absolute power of the R1 section, compared to five frequency ranges with intermediate wave speeds (Alpha 1 and 2, and Beta 1-3). 1: Rest 1, 2: Task 1, 3: Task 2, 4: Task 3, 5: Rest 2

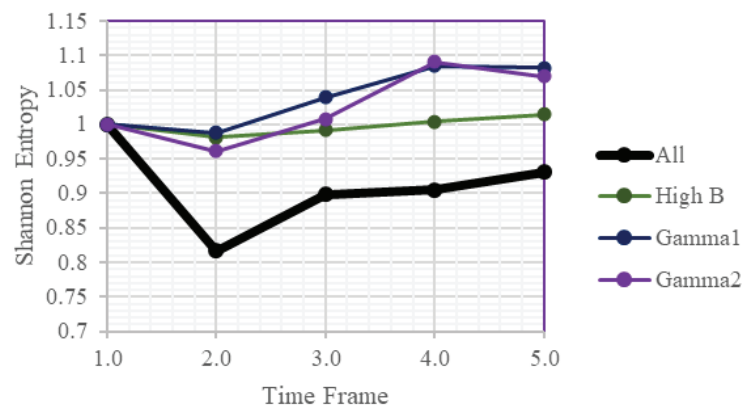


Figure 3. The trend of changes normalized to the total absolute power of the R1 section, compared to three frequency ranges with maximum wave speeds (High Beta, Gamma 1, and Gamma 2). 1: Rest 1, 2: Task 1, 3: Task 2, 4: Task 3, 5: Rest 2.

The minimum entropy values are presented in the following charts. The trend of changes normalized to the total absolute power of the R1 section, compared to the two frequency ranges with the minimum wave speeds (Delta and Theta), shows that the trend of changes up to Task 3 is similar to the trend of total minimum entropy changes (Figure 4). According to Figure 5, in comparison with the four frequency ranges with intermediate wave speeds (Alpha 1 and 2, Beta 1 and 2), the trend of changes up to Task 3

is similar to the trend of total minimum entropy changes. In the case of Alpha 2 and Beta 1 waves, the return of minimum entropy values in Rest 2 to Rest 1 is complete. Regarding the four frequency ranges with maximum wave speeds (High Beta, Gamma 1, and Gamma 2), the trend of changes in Task 1 increasingly deviates from the trend of total minimum entropy changes as wave speed increases. Beta 3 and High Beta waves in Rest 2 tend to approach the values observed in Rest 1.

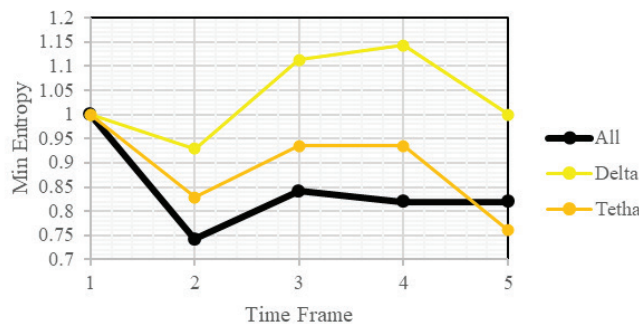


Figure 4. The trend of changes normalized to the total absolute power of the R1 section, compared to the two frequency ranges with the minimum wave speeds (Delta and Theta).

1: Rest 1, 2: Task 1, 3: Task 2, 4: Task 3, 5: Rest 2.

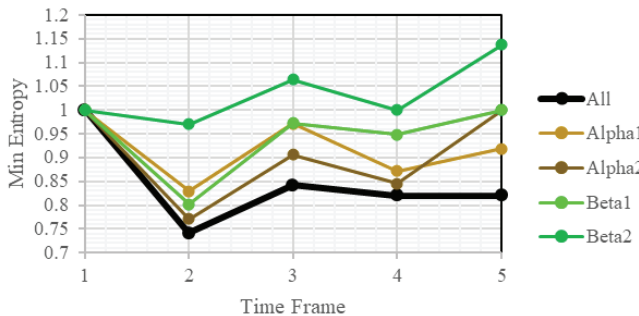


Figure 5. The trend of changes normalized to the total absolute power of the R1 section, compared to the four frequency ranges with intermediate wave speeds (Alpha 1 and 2, Beta 1 and 2).

1: Rest 1, 2: Task 1, 3: Task 2, 4: Task 3, 5: Rest 2.

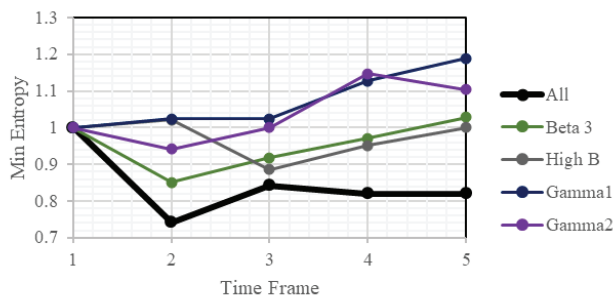


Figure 6. The trend of changes normalized to the total absolute power of the R1 section, compared to the four frequency ranges with maximum wave speeds (Beta3, High Beta, Gamma 1, and Gamma 2).

1: Rest 1, 2: Task 1, 3: Task 2, 4: Task 3, 5: Rest 2

In summary, it can be said that the calculation of entropy provides a useful perspective on the effects of T-Consciousness Fields at the brain level. Initially, these changes offer evidence of information transmission under the influence of the Faradarmani Consciousness Field. In the next step, by comparing different time segments, especially Task 1 (or the onset of the Faradarmani Consciousness Field effect) and Rest 2 (or the declaration of the end of the effect), clear fluctuations are observed, indicating information processing and changes at the brain level.

Acknowledgment

Authors would like to acknowledge the Iranian National Brain Mapping Laboratory (NBML), Tehran, Iran for providing data acquisition service for this research work.

References

- Bein, B. (2006). Entropy. *Best Practice & Research Clinical Anaesthesiology*, 20(1), 101-109. <https://doi.org/10.1016/j.bpa.2005.07.009>
- Delorme, A., & Makeig, S. (2004). EEGLAB: an open source toolbox for analysis of single-trial EEG dynamics including independent component analysis. *Journal of neuroscience methods*, 134(1), 9–21. <https://doi.org/10.1016/j.jneumeth.2003.10.009>
- Keshmiri, S. (2020). Entropy and the Brain: An Overview. *Entropy (Basel, Switzerland)*, 22(9), 917. <https://doi.org/10.3390/e22090917>
- Oostenveld, R., Fries, P., Maris, E., & Schoffelen, J. M. (2011). FieldTrip: Open source software for advanced analysis of MEG, EEG, and invasive electrophysiological data. *Computational intelligence and neuroscience*, 2011, 156869. <https://doi.org/10.1155/2011/156869>
- Sabeti, M., Katebi, S., & Boostani, R. (2009). Entropy and complexity measures for EEG signal classification of schizophrenic and control participants. *Artificial intelligence in medicine*, 47(3), 263–274. <https://doi.org/10.1016/j.artmed.2009.03.003>
- Sadeghijam, M., Talebian, S., Mohsen, S., Akbari, M., & Pourbakht, A. (2021). Shannon entropy measures for EEG signals in tinnitus. *Neuroscience letters*, 762, 136153. <https://doi.org/10.1016/j.neulet.2021.136153>
- Saraiva, P. (2023). On Shannon entropy and its applications. *Kuwait Journal of Science*, 50(3), 194-199. <https://doi.org/10.1016/j.kjs.2023.05.004>
- Shannon, C. E. (1948). A mathematical theory of communication. *The Bell System Technical Journal*, 27(3), 379-423.
- Taheri, M. A., Modarresi-Asem, F., & Semsarha, F. (2022). An Investigation of the Electrical Activity of the Brain during the Treatment with Faradarmani Consciousness Field in the Faradarmangar Population. *The Scientific Journal of CosmoIntel*, 1(2), 22–32. <https://doi.org/10.61450/joci.v1i2.19>

Taheri, M. A., Torabi, S., Nabavi, N., Modarresi-Asem, F., Abbasi Sisara, M., Maftoun, P., & Semsarha, F. (2022a). Task-fMRI Group and Functional Connectivity Analysis of the Brain During Faradarmani Consciousness Field Connection. *The Scientific Journal of Cosmointel*, 1(2), 46–55. <https://doi.org/10.61450/joci.v1i2.29>

Taheri, M.A (2013) Human from another outlook Interuniversal Press; 2nd Edition ISBN-13: 978-1939507006, ISBN- 10: 1939507006

Yuvaraj, R., Murugappan, M., Mohamed Ibrahim, N. et al. (2024). On the analysis of EEG power, frequency and asymmetry in Parkinson's disease during emotion processing. *Behavioral and brain functions*, 10(1), 12. <https://doi.org/10.1186/1744-9081-10-12>

